Preprint 25 September 2017
Accepted by "Physical Chemistry Chemical Physics" (Royal Society of Chemistry, UK) 25/09/2017

Molecular field theory for biaxial nematics formed from liquid crystal dimers and inhibited by the twist-bend nematic

T.B.T. To* and T.J. Sluckin

Mathematical Sciences, University of Southampton, Southampton, SO17 1BJ, United Kingdom

G.R. Luckhurst

Chemistry, University of Southampton, Southampton, SO17 1BJ, United Kingdom

(Dated: September 29, 2017)

Abstract

Liquid crystal dimers with odd spacers are good candidates as materials for biaxial nematic phases (N_B). The dimers are flexible molecules sustaining biaxial conformations, and couplings between the conformational and orientational distributions could be expected to stabilise N_B. We apply a molecular field theory for flexible molecules developed elsewhere to study a simple system made up of dimers composed of two cylindrically symmetric mesogenic groups. Our model allows for two idealised conformations: one linear and one bent at a tetrahedral angle. For a restricted set of chain lengths, the model predicts a first-order reentrant phase transition from the N_B phase into a low temperature uniaxial nematic phase (N_U). However the formation of the biaxial nematic could be blocked by the appearance of a twist-bent nematic.

* Instituto de Física, Universidade Federal Fluminense, Avenida Litorânea s/n, 24210-340 Niterói RJ, Brazil (current address). Email: tungto@if.uff.br

I. INTRODUCTION

Most known nematic liquid crystals are uniaxial (N_U), in which, informally speaking, constituent molecules align one molecular axis to form a single macroscopic director [1]. Over forty years ago, Freiser [2] predicted the possible existence of a biaxial nematic liquid crystal phase (N_B). In this phase, again informally speaking, all three molecular axes align to form three macroscopic directors. Despite a well-attested observation of lyotropic biaxial nematic phases [3], for a long time there was no report of a thermotropic nematic biaxial phase. Following observational reports of such phases (see e.g. [4–8]), there has been a renewal of interest in this field; the subject has been reviewed recently in a book edited by two of the present authors [9].

From a technological viewpoint, the switching of the nematic director by an electric field is the basic working principle of liquid crystal display devices. However, for calamitic molecules, the switching times of the shorter molecular axes have been demonstrated to be much shorter than that of the major axis. This suggests that biaxial nematic phases could possess interesting electro-optical applications [10–12].

Following Freiser [2], several molecular field theories for the elusive N_B phase were proposed. Most such theories assume the constituent molecules to be rigid and to possess D_{2h} symmetry (see e.g. [13–16]). These theories were also validated by computer simulations (see e.g. [17–20]). On the experimental side, the early observations of lyotropic biaxial nematic phases [3] were followed much later by well-publicised reports of the existence of thermotropic biaxial nematic phases in V-shaped nematics [4, 5] and molecular tetrapodes [6–8]. The V-shaped systems [4, 5] have attracted some controversy in the literature (see e.g. [10, 21–23]). In addition, it is now realised that nematics consisting of V-shaped molecules are often susceptible to the formation of the so-called twist-bend nematic phase $N_{\rm TB}$. In this phase, the director forms a tight helical twist of both chiralities [24–26]; this phase may be pre-empting biaxial nematics

in experimental cases. We shall return to this intriguing possibility at the end of our paper in the Discussion.

The N_B phases formed by the tetrapodal systems may be regarded as more but not completely conclusive [27–30], and on the other hand more challenging for theoretical studies. Four flexible chains connect the core with the mesogenic groups, implying a very large number of conformations. This modelling difficulty is also relevant for a number of molecular structures which are highly biaxial in shape and potentially good candidates to stabilise N_B (see e.g. [31]). To address this issue, Luckhurst [31] developed a molecular field theory for N_B formed from flexible molecules. Our paper concerns primarily the application of this theory to a simple system of dimers consisting of two identical uniaxial mesogenic groups connected via a hydrocarbon chain [32].

One appealing strategy to stabilise the N_B phase is simply to form a mixture of rod- and disc-like molecules [33]. However this strategy often seems to fail. Rather than stabilise the N_B phase, the mixture tends to phase separate into two coexisting uniaxial nematic phases, one calamitic and one discotic [34]. However, if in an analogous system, the rod- and disc-like molecules are interconvertible, then the Gibbs phase rule forbids such phase separation. An early attempt at employing this strategy to locate a biaxial nematic phase was made by Vanakaras *et al.* [35] for an interconverting mixture of hard rod-like and plate-like conformers. However, it appears that packing such hard particles created difficulties for the formation of the N_B phase. More recently Teixeira and Masters [36] attempted to solve the same problem using interconverting prolate and oblate spheroids based on an Onsager theory. Unfortunately, in this system, the N_B phase is always unstable with respect to the N_U phase. However, in general, we might expect the presence of biaxial conformers in an interconverting multicomponent system of liquid crystal dimers to stabilise the N_B phase. For example, a lattice system of flexible V-shaped molecules allowing for a continuous range of conformations has been studied by Bates [37] using Monte Carlo simulations. This study indeed finds

that the N_B phase is stabilised in the ground state, and also finds a second biaxial N_B phase near the clearing point. The two N_B phases are separated by a N_U phase rich in rod conformers.

Here we use molecular field theory to study interconverting V-shaped molecules, and we also expect to find a rich phase behaviour. Our goal is to study the effect of the interaction between conformational-orientational distributions and the stability of the biaxial phase. A previous study by Ferrarini *et al.*[32] found that certain mixtures rich in the bent conformer were able to undergo a strong nematic-nematic transition; both nematics being uniaxial. This striking transition occurs because the high-temperature nematic has a low orientational order coming from the high concentration of the bent conformer. As a consequence it can couple to the nematic order and so enhance the concentration of the linear conformer in the low temperature nematic. Likewise, we expect that biaxial order would induce an increase in the mole fraction of the biaxial conformer, and hence stabilise phase biaxiality. Indeed this might have been anticipated for the model system originally studied by Ferrarini *et al.* [32]. However the theory needed to observe the biaxial nematic was not available at the time and it is our intention to remove this omission here.

The plan of the paper is as follows. In Section II we present the theoretical background proposed by Luckhurst [31] for a general system of flexible molecules. This general theory is applied to illustrate our approach for a flexible system having two conformers in Section III. In Section IV, we present the numerical results of our calculations for the flexible system. In Section V, we discuss our results and their relation to other work, in particular to the twist-bend nematic phase. Our conclusions are given in Section 6.

II. THEORETICAL BACKGROUND

A. Basis functions and order parameters

The molecular field theory requires an orientational distribution function $f(\Omega)$ and a set of order parameters. The molecular orientation Ω is parameterised in terms of the three Euler angles α, β, γ which take their conventional meanings (polar angle β and zenithal angles α, γ). The Euler angle α is only required in the spontaneously biaxial phases. A complete theory for biaxial nematics possessing D_{2h} symmetry (i.e. that of a rectangular parallelepiped) formed from molecules with C_{2v} symmetry (that of the letter V) requires four scalar second-rank order parameters. These second-rank order parameters are the same as those for biaxial nematics with D_{2h} symmetry formed from molecules with D_{2h} symmetry. They are denoted as (S, D, P, C) [16, 38], which are orientational averages of basis angular functions (R_S, R_D, R_P, R_C). We follow the notation convention of Teixeira *et al.*[39], but with different scaling (see also Dunmur and Luckhurst [40] and Luckhurst [41]). Some of this material can also be found elsewhere [42]. The functions are:

$$R_S(\Omega) = \frac{1}{2}\left(3\cos^2\beta - 1\right); \tag{1a}$$

$$R_D(\Omega) = \sqrt{\frac{3}{8}}\sin^2\beta\cos 2\gamma; \tag{1b}$$

$$R_P(\Omega) = \sqrt{\frac{3}{8}}\sin^2\beta\cos 2\alpha; \tag{1c}$$

$$R_C(\Omega) = \frac{1}{2}\left(1+\cos^2\beta\right)\cos 2\gamma\cos 2\alpha - \cos\beta\sin 2\gamma\sin 2\alpha. \tag{1d}$$

The order parameters are defined in terms of basis angular function averages:

$$i = \langle R_i \rangle = \int d\Omega f(\Omega) R_i(\Omega), \tag{2}$$

with $i \in \{S, D, P, C\}$. We note that (subject to exchange of axes) in the N_U phase, in general, $S, D \neq 0$, but $C = P = 0$. In biaxial phases all four order parameters in general are non-zero. At the ground state $S = C = 1$ and $D = P = 0$ in the complete order limit.

B. Basic material

We suppose the constituent bent-core molecules possess C_{2v} symmetry. We will refer to them as V-shaped molecules. Thermodynamic quantities, namely the free energy, internal energy, potentials of mean torque, orientational distribution functions and partition functions are formulated per particle. Moreover, the temperature and energy quantities are expressed in non-dimensional units. We denote the internal energy by U, and the potential of mean torque acting on a molecule with orientation Ω by $U(\Omega)$.

Our molecular field theory is an extension of the Maier-Saupe theory which was developed for uniaxial nematics formed from uniaxial molecules. The free energy per particle is given by:

$$A = k_B T \int_\Omega d\Omega f(\Omega) \ln\left(8\pi^2 f(\Omega)\right) - \frac{1}{2}\frac{u_{200}}{v} S^2, \tag{3}$$

where k_B denotes the Boltzmann constant, T is the absolute temperature, u_{200} sets the scale of the molecular anisotropic interaction, and v is the volume of the mesogenic group. Here the inverse volume dependence originates, as Cotter has shown, from statistical mechanical consistency in the molecular field theory [43].

The model combines elements of the molecular field theory of biaxial nematics with C_{2v} and D_{2h} symmetry developed elsewhere [13–15, 44] with the molecular field theory of uniaxial nematics formed from a binary system of interconverting rod-like and tetrahedral V-shaped conformers [45]. At second-rank level, the theories for molecules formed from D_{2h} and C_{2v} symmetry are equivalent. We note that in this sense the

mathematical structure of our model is equivalent to that for a system consisting of uniaxial and biaxial parallelepiped molecules, although the formation of the N_{TB} phase requires a V-shape.

C. Theory of rigid molecules

Here, we discuss the theory for rigid V-shaped molecules composed of two identical arms as a preliminary background before developing the theory for flexible V-shaped molecules in the next Subsection. Following the Maier-Saupe theory, we assume that second-rank order parameters are dominant. Thus the anisotropic internal energy for a rigid molecular system is given by

$$U = U_{\mathrm{anis}} = -\frac{1}{2v}\sum u_{2mn}\langle D^2_{pm}\rangle\langle D^2_{-pn}\rangle, \tag{4}$$

where the $\langle D^2_{pm}\rangle$ are the thermodynamic averages of the Wigner rotation matrices $D^2_{pm}(\Omega)$ (see Section A.2, p. 458 [46]), v is the volume of a mesogenic group. The irreducible supertensor u_{2mn} depends on the properties of two interacting molecules. To simplify the theory, we use the separability approximation [47]:

$$u_{2mn} = u_{2m}u_{2n}. \tag{5}$$

Here, the spherical tensor u_{2m} depends on the molecular structure. For example, if the u_{2mn} are the coefficients in the expansion of the dispersion interaction between two molecules then the u_{2m} are the components of the molecular polarisability tensor (see Eq. (2.234), Section 2.6, p. 98 [46]). For C_{2v} and D_{2h} molecules, this approximation is also in agreement with the so-called geometric mean approximation [13, 14, 48]. This model requires only two order parameters, rather than the full complement of four. These are defined as follows:

$$\mathcal{J}_1 = \langle J_1(\Omega)\rangle = \langle R_S(\Omega) + 2\lambda R_D(\Omega)\rangle = S + 2\lambda D, \tag{6a}$$

$$\mathcal{J}_2 = \langle J_2(\Omega)\rangle = \langle R_P(\Omega) + \lambda R_C(\Omega)\rangle = P + \lambda C, \tag{6b}$$

where λ is the molecular biaxiality parameter. In the I phase both order parameters are zero, in the N_U phase, $\mathcal{J}_1 \neq 0$, but $\mathcal{J}_2 = 0$, while in the N_B phase neither order parameter is zero. The case $\lambda = 0$ corresponds to uniaxial $D_{\infty h}$ molecules.

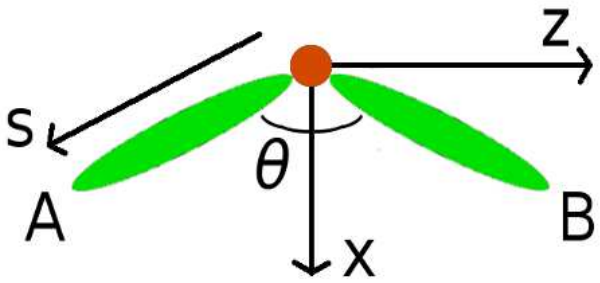

FIG. 1. A sketch of the idealised V-shaped molecule. The axis x points along the bisector of the two axes of the arms. The axis z is in the same plane as the two arm axes and perpendicular to x. The axis s points along an arm. Note that θ here is the full interarm angle between the cylindrical arms A and B.

The value of λ can be related to the shape of V-shaped molecules by the method given by Ferrarini *et al.*[45] and Bates and Luckhurst [47]. In Fig. 1 we show this molecular model which consists of two identical uniaxial arms joined with an interarm angle θ. In this paper we define the molecular coordinate axes as in Fig. 1. The x axis points along the bisector of the two symmetry axes of the arms while the z axis is in the same plane as the two arm axes and the s axis points along the symmetry axis of an arm. Following Eqs. (B10), p. 13 [47], the molecular tensor components u_{2m} are the sum of the contributions from both the two arms. In the principle coordinate axes

shown in Fig. 1 they can be written as

$$u_{20} = \sqrt{\frac{3}{8}}\epsilon(1 + 3|cos\theta|)\sqrt{\phi}, \tag{7a}$$

$$u_{22} = \frac{3}{4}\epsilon(1 - |cos\theta|)\sqrt{\phi}, \tag{7b}$$

where ϵ is the Cartesian tensor component of an arm along the s axis. The value of ϵ can be related to the spherical tensor component of the arm $\tilde{u}_{20}$ by using Eqs. (A.231a, A.231b, A.231c), p. 492 [46] together with the property that the second-rank Cartesian tensor is traceless which gives

$$\epsilon = \sqrt{\frac{2}{3}}\tilde{u}_{20}. \tag{8}$$

ϕ is the volume fraction of a mesogenic group in the molecule [49]. For our model of V-shaped molecules where there are two mesogenic groups, $\phi = 1/2$. Then we can rewrite Eqs. (7) as

$$u_{20} = \frac{1}{2}\tilde{u}_{20}(1 + 3|cos\theta|)\sqrt{\phi}, \tag{9a}$$

$$u_{22} = \frac{1}{2}\sqrt{\frac{3}{2}}\tilde{u}_{20}(1 - |cos\theta|)\sqrt{\phi}. \tag{9b}$$

The expansion of the internal energy (4) with the separability approximation (5) depends on two molecular parameters u_{20} and u_{22}. These molecular parameters depend on those of the arms according to Eq. (9). Thus we shall work, where possible, in non-dimensional quantities, given in terms of their physical quantities by

$$\begin{aligned} T^* &= \frac{vk_BT}{\tilde{u}_{20}^2}; \quad A^* = \frac{vA}{\tilde{u}_{20}^2}; \\ U^* &= \frac{vU}{\tilde{u}_{20}^2}; \quad U^*(\Omega) = \frac{vU(\Omega)}{\tilde{u}_{20}^2}. \end{aligned} \tag{10}$$

The scaled internal energy is given by

$$U^* = \frac{vU}{\tilde{u}_{20}^2} = -\frac{1}{2}\phi g(\theta)^2(\mathcal{J}_1^2 + 2\mathcal{J}_2^2). \tag{11}$$

Here, the parameters are defined as

$$\lambda(\theta) = \frac{u_{22}}{u_{20}} = \sqrt{\frac{3}{2}}\frac{(1+\cos\theta)}{(1-3\cos\theta)}, \tag{12a}$$

and

$$g(\theta) = \frac{u_{20}}{\tilde{u}_{20}} = \frac{1}{2}(1-3\cos\theta). \tag{12b}$$

Here, $g(\theta)$ measures the relative anisotropy between the molecule and a mesogenic group.

The orientational distribution function $f(\Omega)$ is derived by minimising a Helmholtz free energy functional:

$$A^* = -T^* \int d\Omega f(\Omega) \ln\left(8\pi^2 f(\Omega)\right) + U^*. \tag{13}$$

The resulting equilibrium orientational distribution function, $f(\Omega)$, is expressed in terms of the potential of mean torque

$$U^*(\Omega) = -\phi g(\theta)^2\Big(\mathcal{J}_1 J_1(\Omega) + 2\mathcal{J}_2 J_2(\Omega)\Big), \tag{14}$$

and is given by

$$f(\Omega) = Q^{-1}\exp\left[-\frac{U^*(\Omega)}{T^*}\right], \tag{15}$$

where the partition function Q is defined in order to normalise the orientational distribution function such that $\int f(\Omega)d\Omega = 1$:

$$Q = \int d\Omega \exp\left[-\frac{U^*(\Omega)}{T^*}\right]. \tag{16}$$

The phase stability of the system is determined from the equilibrium Helmholtz free energy:

$$A^* = -T^* \log Q - U^*. \tag{17}$$

The phase diagram in Fig. 2 shows the dependence of the scaled transition temperatures on the interarm angle θ for V-shaped molecules; this has been discussed by several

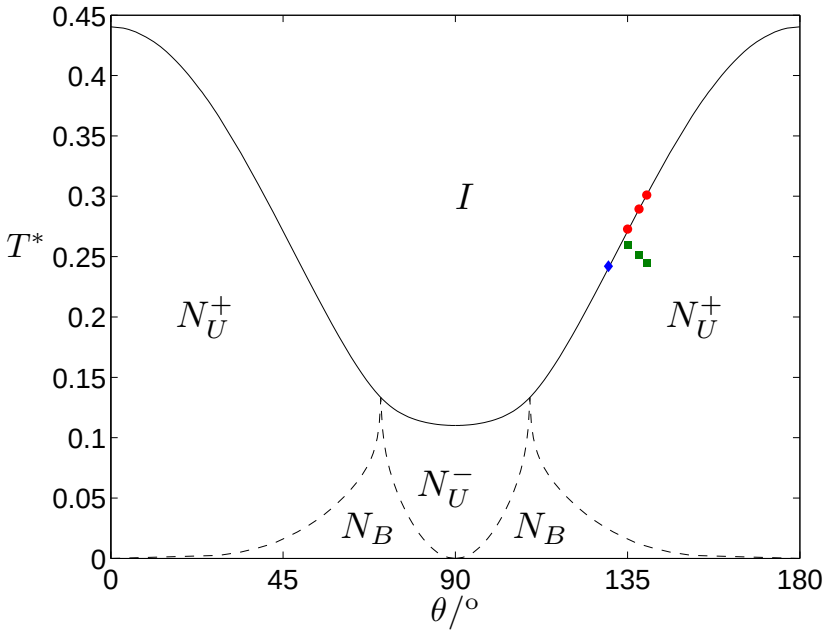

FIG. 2. The scaled transition temperatures as a function of the interarm angle θ for V-shaped molecules. Solid lines: first-order transitions. Dashed lines: continuous transitions. For the V-shaped dimers forming the twist-bend nematic phase ● denotes the $T^*_{N_U-I}$ transition, ■ the $T^*_{N_{\rm TB}-N_U}$ transition and ◆ the $T^*_{N_{\rm TB}-I}$ transition (see Section V B).

authors [10, 45, 47]. Here we use N_U^+ and N_U^- to denote the uniaxial nematic phases formed by aligning the molecular axis z and y (orthogonal to x and z), respectively. Thus N_U^+ is a calamitic uniaxial nematic which exists between the I and N_B phases for $0^\circ < \theta \lesssim 70.5^\circ$ and $109.5^\circ \lesssim \theta < 180^\circ$ (equivalent to $0 < \lambda < 1/\sqrt{6}$). On the other hand, N_U^- is a discotic uniaxial nematic which exists between the I and N_B phases for $70.5^\circ \lesssim \theta \lesssim 109.5^\circ$ (equivalent to $1/\sqrt{6} < \lambda < \sqrt{3/2}$). At the intersection of these parameter ranges, namely $\theta = \theta_c = \cos^{-1}(1/3) \approx (70.5^\circ, 109.5^\circ)$ or $\lambda = 1/\sqrt{6}$ (see also [13–15, 50]), the I phase enters directly into the N_B phase through a continuous phase

transition at the Landau multicritical point. Since the phase diagram is symmetrical about $\theta = 90^{\rm o}$, it suffices to analyze the case $\theta > 90^{\rm o}$.

The stability of the biaxial nematic phase N_B increases relative to that of the uniaxial nematic N_U^- on increasing θ from $90^{\rm o}$ up to the Landau multicritical point at $\theta = \theta_c$. As θ increases away from θ_c the stability of N_B decreases relative to that of N_U^+. Here, the ground state is always N_B. For $\theta \lesssim 100^{\rm o}$ and $\theta \gtrsim 130^{\rm o}$, the N_B phase only intercedes at very low temperature. As θ approaches θ_c the $N_B - N_U$ phase boundary increases gradually in temperature. We note the sharp increase of the $N_B - N_U$ transition temperature in the vicinity of θ_c, indicating the sensitivity of the phase transition to θ at the Landau point. Then at the Landau multicritical point $\theta = \theta_c$, all phases coincide.

D. Theory of multi-conformer systems

In this Subsection we summarise the theory, due to Luckhurst [31], for liquid crystals formed from flexible molecules. In a system of discrete exchanging conformers the total internal energy per particle consists of the anisotropic and the conformational energies

$$U = U_{\rm anis} + U_{\rm conf}. \tag{18}$$

The anisotropic internal energy per particle is given by

$$U_{\rm anis} = -\frac{1}{2}\frac{\phi}{v}\sum p_k p_j u_{2mn}^{kj} \langle D_{pm}^2 \rangle_k \langle D_{-pn}^2 \rangle_j, \tag{19}$$

where p_j denotes the conformational distribution function of conformer j; u_{2mn}^{kj} denotes the component of the interaction supertensors between the two conformers, k and j; $\langle D_{pm}^2 \rangle_k$ denotes the order parameter defined by averaging the corresponding Wigner function with respect to the orientations of conformer k. The conformational energy

per particle can be written as

$$U_{\text{conf}} = \sum p_j \tilde{u}^j_{\text{conf}}, \tag{20}$$

where $\tilde{u}^j_{\text{conf}}$ is defined as the sum of the conformational energy u^j_{conf} and the additional scalar interaction, u^{kj}_0 between two non-identical molecules. According to the Flory RIS model [51], the two bonds which connect to a third bond in the hydrocarbon chain can take one of three states, namely one *trans* and two *gauche* configurations, where the *trans* configuration is taken as the ground state. Thus the conformational energy u^j_{conf} is the sum over the energy difference of all the *gauche* links with respect to their *trans* configuration.

Next, we define the total entropy which has contributions from the conformational and orientational terms

$$\mathcal{S} = -k_B \sum \left\{ p_j \int f_j(\Omega) \ln f_j(\Omega) d\Omega + p_j \ln p_j \right\}. \tag{21}$$

Here, the first term of the sum denotes the orientational entropy and the second term denotes its conformational counterpart.

To find the distribution functions, we minimise the free energy per particle,

$$A = U - T\mathcal{S}, \tag{22}$$

with respect to the distribution functions. The resulting orientational distribution function for a given conformer is written in terms of the potential of mean torque as:

$$f_j(\Omega) = Q_j^{-1} \exp\left(\frac{U_j(\Omega)}{k_B T}\right), \tag{23}$$

where the partition function , Q_j, is defined in order to normalise the orientational distribution function such that $\int f_j(\Omega) d\Omega = 1$,

$$Q_j = \int \exp\left(\frac{U_j(\Omega)}{k_B T}\right) d\Omega. \tag{24}$$

Here, the potential of mean torque for conformer j is given by

$$U_j(\Omega) = -\frac{\phi}{v}\sum p_k u^{kj}_{2mn}\langle D^2_{pm}\rangle_k D^2_{-pn}(\Omega). \tag{25}$$

In addition, the resulting conformational distribution function is given by

$$p_j = Z^{-1}Q_j \exp\left(-\frac{\tilde{u}^j_{\rm conf}}{k_B T}\right). \tag{26}$$

Here, Z denotes the conformational-orientational distribution function

$$Z = \sum_k \exp\left(-\frac{\tilde{u}^k_{\rm conf}}{k_B T}\right) Q_k. \tag{27}$$

Finally, the free energy at equilibrium is given by

$$A = -U_{\rm anis} - k_B T \ln Z, \tag{28}$$

where $U_{\rm anis}$ represents the specifically anisotropic contributions to the free energy, and the isotropic contributions are not relevant for our purposes and is infact contained in Z.

III. THEORY FOR TWO-CONFORMER SYSTEMS

A. Application of the general theory

In this Section we apply the theory developed in Section II to the system of liquid crystal dimers consisting of just two conformations. These, one bent and the other linear, are shown in two dimensions and sketched in Fig. 3, the limitation to just two has the clear merit of simplifying the molecular field calculations. However, it also has a realistic element consistent with the discrete conformations of the Rotational Isomeric State (RIS) model of Flory [51]. For an alkane, having tetrahedral angles, $\cos^{-1}(1/3) \approx 109.5^{\rm o}$, between linked C-C bonds, each of the carbon atoms or methylene

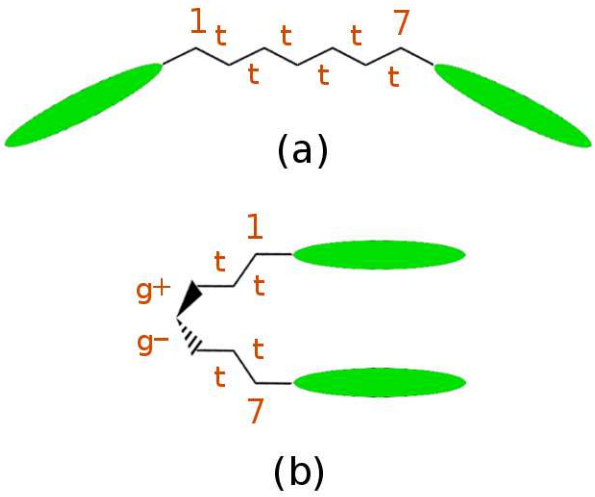

FIG. 3. Two-dimensional sketches of the odd dimer CB7CB in mesogenic conformers with (a) bent (all-trans) and (b) parallel mesogenic groups (hairpin) conformation. In (a), the all-trans conformation of the heptane spacer is (tttttt). In (b), The hairpin conformation with its two gauche states in the centre of the spacer is (ttg^+g^-tt).

groups occupy the sites of part of a diamond lattice. As a result, for a liquid crystal dimer with a heptane spacer, in the all-*trans* form, the *para*-axes of the two mesogenic groups are inclined at the tetrahedral angle. In contrast with two *gauche* links in the centre of the spacer, ttg^+g^-tt, the *para*-axes are found to be parallel to each other giving the hairpin conformation. No other relative orientations are possible and so based on the RIS model the use of just two conformers in our calculations is quite reasonable. The other feature of the model is the probability of these conformers. In the isotropic phase by far the most probable conformer is that which is bent. This situation can change significantly in the nematic phase because of the orientational order which couples to the conformational distribution; as a consequence the probability of the linear or hairpin conformer will grow at the expense of the bent [45].

In our model based on second-rank interactions, there are two potentials of mean torque, given by replacing the dummy subscripts (j,k) in Eq. (25) by (l,b) which represent the linear and bent conformers, respectively. We also use the separability approximation of Eq. (5) [31]

$$u_{2mn}^{kj} = u_{2m}^{k} u_{2n}^{j}. \tag{29}$$

Previous studies by Ferrarini *et al.*[45] and Bates and Luckhurst [47] give us the values for the interaction tensor components in Eqs. (12)

$$g(180^{\mathrm{o}}) = \frac{u_{20}^{l}}{\tilde{u}_{20}} = 4, \tag{30a}$$

$$\lambda(180^{\mathrm{o}}) = \frac{u_{22}^{l}}{u_{20}^{l}} = 0, \tag{30b}$$

$$g(\theta_c) = \frac{u_{20}^{b}}{\tilde{u}_{20}} = 2, \tag{30c}$$

$$\lambda(\theta_c) = \frac{u_{22}^{b}}{u_{20}^{b}} = \frac{1}{\sqrt{6}}. \tag{30d}$$

Thus the explicit expressions of the potentials of mean torque for linear and bent conformers are given by

$$U_l(\Omega)^* = -4\phi \left[\mathcal{J}_1 R_S(\Omega) + 2\mathcal{J}_2 R_P(\Omega)\right], \tag{31a}$$

$$\begin{aligned} U_b(\Omega)^* = -2\phi \Bigg[& \mathcal{J}_1 \left(R_S(\Omega) + \frac{2}{\sqrt{6}} R_D(\Omega) \right) \\ & + 2\mathcal{J}_2 \left(R_P(\Omega) + \frac{1}{\sqrt{6}} R_C(\Omega) \right) \Bigg]. \end{aligned} \tag{31b}$$

Here, the order parameters $\mathcal{J}_1$ and $\mathcal{J}_2$ are the linear combinations of the order parameters of the linear and bent conformers

$$\begin{aligned} \mathcal{J}_1 &= p_l S_l + \frac{1}{2} p_b \left(S_b + \frac{2}{\sqrt{6}} D_b \right), \\ \mathcal{J}_2 &= p_l P_l + \frac{1}{2} p_b \left(P_b + \frac{1}{\sqrt{6}} C_b \right), \end{aligned} \tag{32}$$

where

$$i_l = \langle R_i \rangle_l = \int d\Omega f_l(\Omega) R_i(\Omega), \qquad i = S, P,$$
$$i_b = \langle R_i \rangle_b = \int d\Omega f_b(\Omega) R_i(\Omega), \qquad i = S, D, P, C. \tag{33}$$

The distribution functions for the linear and bent conformers are given by:

$$f_{l/b}(\Omega) = Q_{l/b}^{-1} \exp\left(\frac{U_{l/b}(\Omega)}{k_B T}\right), \tag{34}$$

where the partition functions, $Q_{l/b}$, are defined to normalise the distribution functions such that $\int f_{l/b}(\Omega) d\Omega = 1$,

$$Q_{l/b} = \int \exp\left(\frac{U_{l/b}(\Omega)}{k_B T}\right) d\Omega. \tag{35}$$

The mole fractions of the two conformers in the isotropic phase are related to the scaled internal energy difference between them (see Eq. (26)) by

$$p_b^0 = \frac{\exp\left(\frac{\Delta E^*}{T^*}\right)}{\left[1 + \exp\left(\frac{\Delta E^*}{T^*}\right)\right]}, \tag{36}$$

where $\Delta E^* = v \Delta E / \tilde{u}_{20}^2$ and the energy difference is defined as

$$\Delta E = (\tilde{u}_{\rm conf}^l - \tilde{u}_{\rm conf}^b). \tag{37}$$

In the nematic phase, the mole fraction of the bent conformer is given by (see Eq. (26))

$$p_b = \frac{\exp\left(\frac{\Delta E^*}{T^*}\right) Q_b}{\left[Q_l + \exp\left(\frac{\Delta E^*}{T^*}\right) Q_b\right]}. \tag{38}$$

We note that, $p_l + p_b = 1$. The variation of the conformational distribution of the bent conformer in the mesophase can be derived from Eq. (36) and Eq. (38)

$$p_b = \frac{p_b^0 Q_b}{(p_b^0 Q_b + p_l^0 Q_l)}. \tag{39}$$

Finally, the scaled free energy at equilibrium is given by (see Eq. (28))

$$A^* = 2\phi\left(\mathcal{J}_1^2 + 2\mathcal{J}_2^2\right) - T^* \ln\left(Q_l + \frac{p_b^0}{p_l^0} Q_b\right). \tag{40}$$

Now we have a theory with two self-consistent equations for $(\mathcal{J}_1, \mathcal{J}_2)$ given in Eqs. (32). On the right-hand-side of Eqs. (32), $\mathcal{J}_1$ and $\mathcal{J}_2$ appear inside the potential of mean torque given in Eqs. (31). Each dimeric system is characterised by a value of ΔE^*. The equilibrium state of a system at a given scaled temperature T^* is determined by the solution to Eqs. (32) that gives the lowest free energy (Eq. (40)).

B. Method

Rather than solve Eqs. (32) directly, we minimise the Helmholtz free energy in Eq. (40). The first derivatives of this equation are the self-consistent Eqs. (32). We note that there are some subtle analytic points, which are addressed, for example by Katriel *et al.*[52]. Strictly speaking this procedure is not valid everywhere for finding minimisers of $A[f(\Omega)]$. We note that Eqs. (32) describe both the minima and the saddle points of the Helmholtz free energy in Eq. (40). Thus, in cases where Eq. (40) has saddle points, the method of minimising it is invalid and we have to resort to solving Eqs. (32) directly. However, the minimisation method is valid for finding stationary points. In the region of interest the method also suffices for determining the present quantities of interest.

The procedure determines the equilibrium order parameters $(\mathcal{J}_1, \mathcal{J}_2)$ at a given temperature. The minimisation uses the MATLAB function fmincon and iterates toward a solution using a quasi-Newton method. The phase transitions are found by determining $(\mathcal{J}_1, \mathcal{J}_2)$, as a function of T^*. The first-order transition is located when there is a discontinuous change in the order parameters as a function of T^*.

IV. NUMERICAL RESULTS

A. Phase diagram

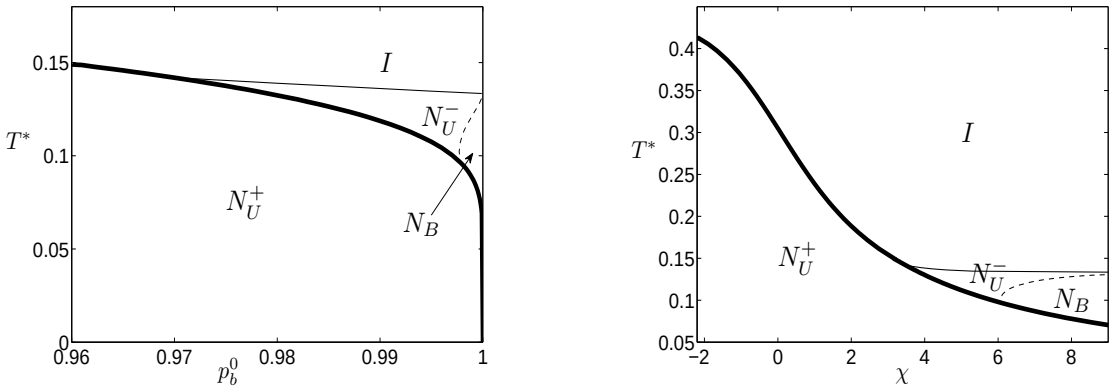

(a) (b)

FIG. 4. Approximate phase diagrams obtained by fixing $\chi = \Delta E^*/T^*$ with respect to T^*. (a): Transition temperatures as a function of the mole fraction p_b^0 in the isotropic phase. (b): Equivalent to (a), but now using χ as the abscissa. We convert p_b^0 into χ using Eq. (41). Lines: thick-solid: first-order transitions; thin-solid: weakly first-order transition; dashed: continuous phase transitions.

We see from Eq. (36) that the conformational distribution in the isotropic phase p_b^0 depends on the energy difference between the two conformers ΔE^* and the scaled absolute temperature T^* through the Boltzmann factor. In the nematic phases, as shown in Eq. (38), the conformational distribution also depends on the orientational orderings of the two conformers via the partition functions $Q_{l/b}$. We shall perform two sets of calculations to determine two phase diagrams. In the first set of calculations we approximate p_b^0 to be independent of temperature. In other words, $\Delta E^*/T^* = \chi$ is

regarded as independent of T^*. Thus we can write

$$p_b^0 = \frac{\exp \chi}{1 + \exp \chi}. \tag{41}$$

The free energy in Eq. (40) is minimised for selected values of $0 \leq p_b^0 \leq 1$. Using this approximation we can make comparison with the previous work by Ferrarini *et al.*[32]. In addition, this approximation gives us an estimate for the range of values of ΔE^* which may stabilise the N_B phase. After we have this estimated range of ΔE^*, we remove the assumption that $\Delta E^*/T^* = \chi$ is independent of T^* and we let p_b^0 vary with T^* as in Eq. (36). Then we minimise the free energy in Eq. (40) with p_b^0 given in Eq. (36) for our estimated range of ΔE^* which stabilises the N_B phase.

Fig. 4a shows the approximate phase diagram as we assume p_b^0 to be independent of T^*. We use N_U^+ and N_U^- to denote the uniaxial nematic phases rich in linear and bent conformers, respectively. The ground state for this system is always a calamitic uniaxial nematic N_U^+. For $p_b^0 \lesssim 0.97$, the $N_U^+ - I$ transition temperature decreases as p_b^0 increases, but there are no extra phases. For $0.97 \lesssim p_b^0 \lesssim 0.9978$, the onset temperature of the N_U^+ phase continues to decrease, but now a discotic uniaxial nematic N_U^- phase is interposed between the I and the N_U^+ phases. The $N_U^- - I$ transition is weakly first order and the $N_U^+ - N_U^-$ transition is first order. These phenomena have been discussed by Ferrarini *et al.*[32] in their study of uniaxial nematics formed from liquid crystal dimers. In our calculation we find a small region of biaxial nematic N_B for $0.9978 \lesssim p_b^0 < 1$. The $N_B - N_U^-$ transition is continuous whereas the $N_U^+ - N_B$ transition is first order. The second phenomenon may be analogous to results found by Ferrarini *et al.*[32], in which the most bent conformers convert into linear conformers. This causes the phase to become calamitic uniaxial. We will address this issue in the next Subsection.

The corresponding parameter range for ΔE^* can be estimated approximately by converting the phase diagram in Fig. 4a from p_b^0 space into χ parameter space using Eq. (41). The resulting phase diagram is shown in Fig. 4b. We see that N_B exists

for $\chi \gtrsim 6$ and $T^* \approx 0.1$. Thus we expect that the N_B phase will be found for $\Delta E^* = \chi \cdot T^* \gtrsim 6 \cdot 0.1 = 0.6$ and so $\Delta E^* \gtrsim 0.6$.

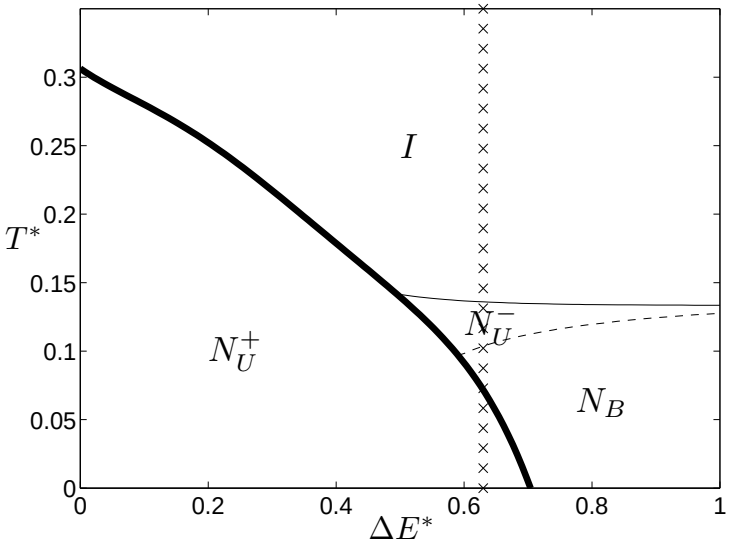

FIG. 5. Phase diagram, showing phases as a function of the scaled conformational energy difference ΔE^* between linear and bent conformers. Lines: thick-solid: first-order transitions; thin-solid: weakly first-order transition; dashed: continuous phase transitions. Vertical crosses: temperature range over which the order parameters and the conformational distribution function shown in Figs. 6 were calculated.

We can now remove the assumption that $\chi = \Delta E^*/T^*$ is independent of T^* and we find the phase diagram by varying ΔE^* from 0 to 1. The resulting diagram is given in Fig. 5. Several features found in Fig. 4b are still preserved in Fig. 5. First, the $N_U^+ - I$ phase transition is first order for $\Delta E^* \lesssim 0.5$. Secondly, the N_U^- phase exists in between the I and the N_B phase; the $N_U^- - I$ transition is weakly first order and the $N_U^+ - N_U^-$ transition is first order. Third, the $N_B - N_U^-$ transition is continuous whereas the $N_U^+ - N_B$ transition is first order. However, a difference between Fig. 5 and Fig. 4b

is that the ground state is N_U^+ only for $\Delta E^* \lesssim 0.7$. For $\Delta E^* \gtrsim 0.7$, the ground state is N_B; thus in this case the large value of ΔE^* does not allow a conversion of the bent conformer into the linear and the ground-state equilibrium at low temperature remains N_B.

B. Coupling of conformational and orientational distributions

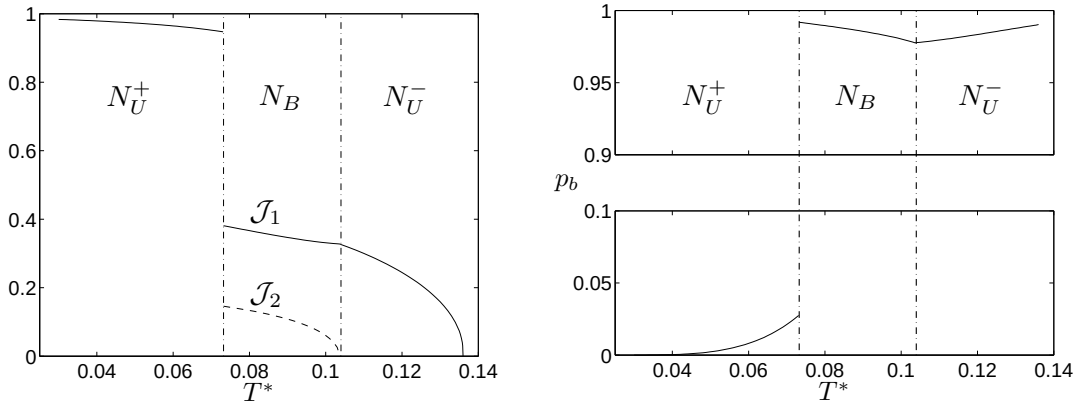

FIG. 6. (a): order parameters $(\mathcal{J}_1, \mathcal{J}_2)$; (b) conformational distribution function of the bent conformer p_b. Both quantities are functions of the scaled temperature T^* for $\Delta E^* = 0.63$, i.e along the crossed line in Fig. 5. Lines in (a): solid: $\mathcal{J}_1$; dashed: $\mathcal{J}_2$. Note anomalous scale in (b), showing that $p_b \ll 1$ in the N_U^+ low temperature phase, whereas $p_l \ll 1$ in the N_B and N_U^- phases; see Fig. 5.

A previous study by Ferrarini *et al.*[32] has analyzed the coupling between the conformational and orientational distributions for two phase sequences $N_U^+ - I$ (for $\Delta E^* \lesssim 0.5$) and $N_U^+ - N_U^- - I$ (for $0.5 \lesssim \Delta E^* \lesssim 0.6$). Here we investigate this coupling for the N_B phase in order to analyse this phase stability. In particular, we want to understand

the $N_B - N_U$ reentrance behaviour for the phase sequence $N_U^+ - N_B - N_U^- - I$ for $0.6 \lesssim \Delta E^* \lesssim 0.7$. Thus in Fig. 6 we show the order parameters $(\mathcal{J}_1, \mathcal{J}_2)$ (see Fig. 6a) and the conformational distribution function of the bent conformer p_b (see Fig. 6b) as functions of the scaled temperature T^* for $\Delta E^* = 0.63$.

The figures show that the mole fraction of the bent conformer decreases in the N_U^- phase and increases in the N_B phase. Equivalently, the biaxial bent conformer is preferentially stabilised in the N_B phase. But at a low temperature $T^* \approx 0.073$, there is a first-order transition to a N_U^+ phase rich in linear conformers. A significant proportion of the bent conformer converts to the linear configuration, there is a jump in the order parameter $\mathcal{J}_1$, and the biaxial order parameter $\mathcal{J}_2$ necessarily suddenly vanishes. As expected, the mole fraction of the bent conformer continues to decrease in the N_U^+ phase as the order parameter $\mathcal{J}_1$ increases. In contrast, the first-order $N_U^+ - N_B$ transition does not occur for $\Delta E^* \gtrsim 0.7$ and so in this case p_b continues to increase in the N_B phase and tends to 1 as the temperature is lowered. However, the underlying reason for the reentrant behaviour, i.e. the low temperature reappearance of a uniaxial phase, remains unclear.

V. DISCUSSION

A. Biaxial nematics

A previous analysis by Ferrarini *et al.*[45] for the phase sequences $N_U^+ - I$ and $N_U^+ - N_U^- - I$ shows that the linear conformation is more favoured than the bent counterpart in the uniaxial phase. Here we have further confirmed this phenomena for the phase sequences that include N_B which is shown in Fig. 6. That is, as expected, in the uniaxial phases, the mole fraction of the linear conformer increases as the uniaxial order parameter $\mathcal{J}_1$ increases. Moreover, Fig. 6 shows that the mole fraction of the bent

conformer increases in the N_B phase as the biaxial order parameter $\mathcal{J}_2$ increases. This confirms our expectation that the biaxial order induces an increase in the concentration of the biaxial conformer.

Our theory is also related to recent work by Teixeira and Masters [36] (TM), who modelled a binary system of interconverting uniaxial rod-like and disc-like ellipsoids using an Onsager-like approach. By comparison, the present work develops a Maier-Saupe-like theory for a biaxial nematic phase formed from a binary system of two nematogenic interconverting conformers, and models liquid crystal dimers, thus extending the model of Ferrarini *et al.* [32]. We note that real dimeric systems with long spacers possess, of course, a large number of conformer shapes. Our model system, in which one conformer is uniaxial and rod-like while the other possesses the maximum biaxiality with an interarm angle $\theta \approx 109.5^{\circ}$, merely corresponds to the two extreme liquid crystal dimer conformers. Intuition nevertheless suggests that this model will be sufficient to yield qualitatively sensible results.

Although the TM methodology is different from ours (Onsager vs. Maier-Saupe), and the systems are also different (ellipsoids vs. dimers), nevertheless some comparison is possible. In our model the uniaxial disc-like conformer would be equivalent to a molecule with an interarm angle θ of 90°. TM found that the N_B phase is always unstable with respect to the N_U phases. A plausible, if preliminary, inference of a comparison of our study with that of TM is thus that the presence of a biaxial phase requires a biaxial component; the mixture of uniaxial prolate and oblate conformations appears to be less efficient to stabilise N_B phase.

A final theoretical connection is with recent results from lattice Monte Carlo simulations by Bates [37]. He studied a system of V-shaped molecules which can adopt a continuous range of conformations with different interarm angles, but having a preferred value. The conformational distribution varies according to a harmonic bending potential $U_i = \epsilon_k(\theta - \theta_0)^2$ which depends on the interarm angle where ϵ_k is the stiffness

of the bending potential and θ_0 is the preferred interarm angle. The V-shaped molecules interact via a simple Maier-Saupe potential between the molecular arms. Thus ϵ_k plays a role analogous to ΔE in our case. In addition, the bending stiffness and temperature is scaled with the interaction tensor along the arm ϵ_{AA}, which is equivalent to $\tilde{u}_{20}^2$ in our case. Thus the scaled bending stiffness $\epsilon_K = \epsilon_k/\epsilon_{AA}$ plays a role analogous to ΔE^* in our case and they are both nondimensional quantities. However these quantities are not exactly equivalent since our model is discrete with just two values whereas that of Bates is continuous and with only one extreme value.

However, it seems that the continuous conformational distribution causes the phase topology to be different from that shown in our phase diagram (see Fig. 5). For $\theta_0 = \theta_c \approx 109.5^{\circ}$, the phase sequence $N_B - I$ was observed for large $\epsilon_K \gtrsim 1000$, as we would expect for very large ΔE^*. For smaller ϵ_K, the N_U^+ phase is inserted between the N_B and the I phases, in contrast to our results for intermediate ΔE^* where the N_U^- phase is found. For a smaller preferred angle $\theta_0 = 100^{\circ}$, the N_U^- phase is found between the N_B and the I phase at intermediate and large $\epsilon_K \gtrsim 11$. For $8 \lesssim \epsilon_K \lesssim 11$, the $N_U^+ - N_U^-$ transition is observed, similar to our results. Moreover, in the simulations by Bates, the ground state is always N_B, in contrast to our results. This may be because the conformational distribution is continuous which allows for more biaxial conformers to be present in the system. Further studies are required to elucidate the precise reasons for the differences between Bates' results and our own.

Among the low molar mass systems that are claimed to form thermotropic biaxial nematics, tetrapodes [6–8] seems to have been the most widely accepted (but note refs [27–30] for alternative views). However, modelling this system is a challenge due to the flexibility of the four flexible chains connecting the four mesogenic groups. This modelling challenge has been addressed for uniaxial nematics [53]. Thus our future work will involve modelling N_B phases formed from tetrapodes based on the combination of our work in this paper and the numerical method for uniaxial nematics formed from

tetrapodes [53] using the theory developed by Luckhurst [31].

B. Twist-bend nematics

We now return to our original idea that although rigid V-shaped molecules may form the biaxial nematic phase there is the possibility that this phase might be blocked by the formation of the twist-bend nematic phase. It is, however, necessary to quantify this notion by estimating the transition temperature at which this new nematic phase might be formed by using the same temperature scale as that in Fig. 2. In fact this is possible because a molecular field theory of the twist-bend nematic phase formed by rigid V-shaped molecules has been developed by Greco *et al.* using a generalisation of the Maier-Saupe theory [54]. As for the model described in Section 2.3 the rigid molecules are V-shaped with an angle, θ, between the two uniaxial mesogenic arms. To the microscopic orientational order parameter $\langle P_2 \rangle$ for each arm are added two macroscopic order parameters to describe the heliconical structure of the $N_{\rm TB}$ phase. One is the pitch, p, of the helix and the other is the tilt angle between the helix axis and the director, θ_0. To place these parameters in their proper context we note that in the standard nematic phase $\langle P_2 \rangle \neq 0$, $p \rightarrow \infty$, and/or $\theta_0 = 0$ whereas in the twist-bend nematic phase the helical pitch is finite, the director makes a non-zero angle with the helical axis and $\langle P_2 \rangle \neq 0$. As with the theory described in Section 2.3 the strength of the anisotropic interaction of each mesogenic arm of the V is denoted by $\tilde{u}_{20}^2$ and the scaled temperature, T^*, is $vk_BT/\tilde{u}_{20}^2$. The variable of special interest to us is the angle θ between the two arms of the molecular V but the range of values studied so far is quite small [54, 55] having been chosen to exhibit phase sequences and transition temperatures analogous to those observed experimentally. For example with θ of 140° the phase sequence is $N_{\rm TB} - N_U - I$ with a long nematic range while for the slightly smaller value of 135° the phase sequence is the same but the nematic range is much

smaller. More interestingly, a further reduction of the value for θ to 130° the nematic phase is removed from the phase sequence giving a transition from the isotropic phase directly to the twist-bend nematic phase. While the sequence $N_{\rm TB} - N_U - I$ is quite common the $N_{\rm TB} - I$ transition has only been observed relatively recently [56–58]. The scaled transition temperatures, $T^*_{N_U-I}$, $T^*_{N_{\rm TB}-N_U}$ and $T^*_{N_{\rm TB}-I}$ available for a range of interarm angles are shown in Figure 2 as a function of the angle θ by the points (●), (■) and (◆), respectively. What we find is that the four transitions to the twist-bend nematic phase occur above that to the biaxial nematic phase showing that for this choice of interarm angles the formation of the N_B phase would indeed be blocked by the $N_{\rm TB}$.

It is perhaps more interesting to see how the transition to the $N_{\rm TB}$ phase changes with respect to T_{N_U-I} for changes in the interarm angle. As we might expect as θ decreases from 140° so the nematic-isotropic transition temperatures shown as the three red circles also decrease. In contrast the twist-bend transition temperatures shown by the green squares increase. The reduction in T_{N_U-I} occurs because of the increased molecular biaxiality or curvature with the decrease in the interarm angle. In contrast as the angle decreases and the curvature grows so too does $T_{N_{\rm TB}-N_U}$. These two changes reduce the nematic range and eventually the twist-bend nematic phase is formed directly from the isotropic phase. We also note that the $N_{\rm TB} - I$ transition falls on the $N_U - I$ phase boundary which may simply be a coincidence. To explore this behaviour further we exploit the proposed analogy between the twist-bend nematic phase and the smectic A phase (SmA) [59]. As we have seen the driving force for the $N_{\rm TB}$ is the curvature or interarm angle. For the SmA it is the molecular inhomogeneity which is related to the length of the terminal chain attached to the aromatic mesogenic group. As the inhomogeneity increases so the tendency to form the SmA phase grows and the $N - I$ transition temperature falls. As experiment shows the boundary between the isotropic phase with either the nematic or the smectic A phase is essentially continuous [60]. In

addition the phase boundary between the N and SmA phases is discontinuous with the boundary to the isotropic phase meeting at the Sm$A - N - I$ triple point. Such behaviour is in good accord with what is predicted for the $N_{\rm TB} - N - I$ phases, clearly supporting our understanding of the phase behaviour of the twist-bend nematic phase as the molecular curvature changes in terms of the analogy between the behaviour of the $N_{\rm TB}$ and SmA phases. We note that although for rigid V-shaped molecules the twist-bend nematic can block the formation of the biaxial nematic phase we cannot say that this will be the case for flexible liquid crystal dimers. To do this we need to extend the theory for the $N_{\rm TB}$ to flexible molecules and this is certainly a non-trivial task which we choose to postpone.

VI. CONCLUSIONS

Our model for flexible, odd liquid crystal dimers has allowed the propensity to form the N_B phase to be investigated. A molecular property of some significance is the energy difference between the linear and bent conformers, and as ΔE^* increases so the probability for the bent conformer grows. Consequently the propensity for the formation of the biaxial nematic phase should also increase. These features of the phase behaviour are clearly apparent in Fig. 5. For small values of ΔE^* the dominance of the uniaxial nematic phase composed largely of the linear conformer N_U^+ is seen. However the stability of this phase with respect to the isotropic decreases as the value of ΔE^* increases and the N_U^- phase rich in the bent conformer appears below the isotropic and above the N_U^+ phase. Its appearance corresponds to a nematic-nematic phase transition; both phases are uniaxial and the difference between them is in the molecular structure. At a slightly higher value of the conformational energy difference the desired biaxial nematic phase appears below the N_U^- phase. As the value of ΔE^* grows further so the width of the N_U^- phase decreases slightly but eventually, with

further increase in ΔE^*, the biaxial nematic phase should be formed directly from the isotropic phase. We can also see that for a small range of ΔE^* below the N_B phase the N_U^+ reappears corresponding, in effect, to a re-entrant nematic phase.

Our results can also provide us with access to the orientational order parameters characteristic of the phases, the uniaxial, $\mathcal{J}_1$, and the biaxial, $\mathcal{J}_2$, and their variation with respect to T^*. To achieve this it is convenient and realistic to fix the conformational energy difference, ΔE^*; in Fig. 6a the energy difference is fixed at 0.63. This value then demands, as we have seen in Fig. 5, that the dimer exhibits the three nematic phases N_U^-, N_B and N_U^+. The temperature variations of the order parameters given in Fig. 6a are consistent with these results. Thus at high temperatures, just above T^* of ~ 0.136, we see that both order parameters are zero as required for the isotropic phase. Then, at T^* of 0.136, there is a small jump in $\mathcal{J}_1$ to about 0.05 corresponding to a very weak first order phase transition; for comparison we note that for a nematogen of uniaxial, rod-like molecules the jump at the nematic-isotropic transition would be 0.429. As expected the biaxial order parameter, $\mathcal{J}_2$, is zero in the N_U^- phase. But then at the lower temperature of ~ 0.104 there is a reduction in the slope of $\mathcal{J}_1$ which corresponds to a second order phase transition. This is to the biaxial nematic phase as the continuous growth of the biaxial order parameter $\mathcal{J}_2$ demonstrates; the nature of the $N_U^- - N_B$ transition also demonstrates that the transition is second order in character. Perhaps surprisingly when the temperature has decreased to 0.073 the biaxial order parameter decreases to zero showing that the N_B phase has undergone a first order transition to the uniaxial nematic N_U^+. Even more striking is that at the transition the uniaxial order parameter has increased to a value somewhat greater than 0.9. This is clearly a very strong first order phase transition and quite unlike that found for the transition to the N_B phase from the N_U^- phase. This qualitative difference in behaviour is associated with the significant change in the conformational distribution when N_U^+ is formed with its high concentration of the linear conformer. Analogous behaviour has

been found for the nematic-nematic transition also predicted to be exhibited by odd liquid crystal dimers [32]. However, the biaxial nematic phase was not predicted for this system because the molecular field theory did not include the order parameter for phase biaxiality.

ACKNOWLEDGMENTS

TBTT acknowledges financial support from the School of Mathematical Sciences, University of Southampton, through a School Ph.D. Studentship. We are grateful to Professor Ferrarini (University of Padua, Italy) for generously sharing her results from the extended molecular field calculations involving the N_{TB} phase and discussing them with us.

---

[1] F. C. Frank, Liquid Crystals, Proc. International Liquid Crystals Conference, Bangalore, Ed. S. Chandrasekhar, Heyden & Sons Ltd., December 1979, London, 1980, pp. 1-6.

[2] M. J. Freiser, Phys. Rev. Lett. **24**, 1041 (1970).

[3] L. J. Yu and A. Saupe, Phys. Rev. Lett. **45**, 1000 (1980).

[4] L. A. Madsen, T. J. Dingemans, M. Nakata, and E. T. Samulski, Phys. Rev. Lett. **92**, 145505 (2004).

[5] B. R. Acharya, A. Primak, and S. Kumar, Phys. Rev. Lett. **92**, 145506 (2004).

[6] K. Merkel, A. Kocot, J. K. Vij, R. Korlacki, G. H. Mehl, and T. Meyer, Phys. Rev. Lett. **93**, 237801 (2004).

[7] J. L. Figueirinhas, C. Cruz, D. Filip, G. Feio, A. C. Ribeiro, Y. Frère, T. Meyer, and G. H. Mehl, Phys. Rev. Lett. **94**, 107802 (2005).

[8] K. Neupane, S. W. Kang, S. Sharma, D. Carney, T. Meyer, G. H. Mehl, D. W. Allender, S. Kumar, and S. Sprunt, Phys. Rev. Lett. **97**, 207802 (2006).

[9] G. R. Luckhurst and T. J. Sluckin (eds.), Biaxial Nematic Liquid Crystals: Theory, Simulation and Experiment, John Wiley & Sons, 2015.

[10] G. Luckhurst, Thin Solid Films **393**, 40 (2001), proceedings from the 4th International Conference on Nano-Molecular Electronics.

[11] J. H. Lee, T. K. Lim, W. T. Kim, and J. I. Lin, J. Appl. Phys. **101**, 034105 (2007).

[12] R. Berardi, L. Muccioli, and C. Zannoni, J. Chem. Phys. **128**, 024905 (2008).

[13] N. Boccara, R. Mejdani, and L. De Seze, J. Phys. France **38**, 149 (1977).

[14] D. K. Remler and A. D. J. Haymet, J. Phys. Chem. **90**, 5426 (1986), http://dx.doi.org/10.1021/j100412a106.

[15] A. M. Sonnet, E. G. Virga, and G. E. Durand, Phys. Rev. E **67**, 061701 (2003).

[16] R. Rosso, Liq. Cryst. **34**, 737 (2007), http://dx.doi.org/10.1080/02678290701284303.

[17] G. Luckhurst and S. Romano, Molecular Physics **40**, 129 (1980), http://dx.doi.org/10.1080/00268978000101341.

[18] F. Biscarini, C. Chiccoli, P. Pasini, F. Semeria, and C. Zannoni, Phys. Rev. Lett. **75**, 1803 (1995).

[19] G. De Matteis, S. Romano, and E. G. Virga, Phys. Rev. E **72**, 041706 (2005).

[20] R. Berardi, L. Muccioli, S. Orlandi, M. Ricci, and C. Zannoni, J. Phys. Condens. Matter **20**, 463101 (2008).

[21] V. Görtz and J. W. Goodby, Chem. Commun. , 3262 (2005).

[22] B. Senyuk, H. Wonderly, M. Mathews, Q. Li, S. V. Shiyanovskii, and O. D. Lavrentovich, Phys. Rev. E **82**, 041711 (2010).

[23] Y.-K. Kim, M. Majumdar, B. I. Senyuk, L. Tortora, J. Seltmann, M. Lehmann, A. Jakli, J. T. Gleeson, O. D. Lavrentovich, and S. Sprunt, Soft Matter **8**, 8880 (2012).

[24] I. Dozov, Europhys. Lett. **56**, 247 (2001).

[25] M. Cestari, S. Diez-Berart, D. A. Dunmur, A. Ferrarini, M. R. de la Fuente, D. J. B. Jackson, D. O. Lopez, G. R. Luckhurst, M. A. Perez-Jubindo, R. M. Richardson, J. Salud, B. A. Timimi, and H. Zimmermann, Phys. Rev. E **84**, 031704 (2011).

[26] S. M. Shamid, S. Dhakal, and J. V. Selinger, Phys. Rev. E **87**, 052503 (2013).

[27] F. Bisi, G. R. Luckhurst, and E. G. Virga, Phys. Rev. E **78**, 021710 (2008).

[28] G. R. Luckhurst, "Thermotropic biaxial nematics: An enduring challenge?" *Erice School on Liquid Crystal Phases and Nano-Structures 2008* (2008), (accessed September 2017).

[29] G. R. Luckhurst, B. A. Timimi, and G. H. Mehl, "A novel and potential biaxial liquid crystal phase formed by an organo-silicon tetrapode. a deuterium nmr investigation," Invited poster in *3rd International Symposium on the Manipulation of Advanced Smart Materials, Osaka 2010* (2010), (accessed September 2017).

[30] Y.-K. Kim, B. Senyuk, S.-T. Shin, A. Kohlmeier, G. H. Mehl, and O. D. Lavrentovich, Soft Matter **10**, 500 (2014).

[31] G. R. Luckhurst, Liq. Cryst. **36**, 1295 (2009), http://dx.doi.org/10.1080/02678290903138729.

[32] A. Ferrarini, G. R. Luckhurst, P. L. Nordio, and S. J. Roskilly, Chem. Phys. Lett. **214**, 409 (1993).

[33] D. W. Bruce, The Chemical Record **4**, 10 (2004).

[34] P. Palffy-Muhoray, J. R. de Bruyn, and D. A. Dunmur, J. Chem. Phys. **82**, 5294 (1985).

[35] A. G. Vanakaras, A. F. Terzis, and D. J. Photinos, Molecular Crystals and Liquid Crystals Science and Technology. Section A. Molecular Crystals and Liquid Crystals **362**, 67 (2001), http://dx.doi.org/10.1080/10587250108025760.

[36] P. I. C. Teixeira and A. J. Masters, Phys. Rev. E **92**, 062506 (2015).

[37] M. A. Bates, Phys. Rev. E **74**, 061702 (2006).

[38] J. P. Straley, Phys. Rev. A **10**, 1881 (1974).

[39] P. I. C. Teixeira, M. A. Osipov, and G. R. Luckhurst, Phys. Rev. E **73**, 061708 (2006).

[40] D. A. Dunmur and G. R. Luckhurst, "Handbook of liquid crystals," in Handbook of Liquid Crystals, Vol. 2 (ed. J. W. Goodby, P. J. Collings, T. Kato, C. Tschierske, H. F. Gleeson and E. P. Raynes, Wiley-VCH, 2014) Chap. 1, pp. 1–39.

[41] G. R. Luckhurst, "Biaxial nematic liquid crystals: Theory, simulation and experiment," (ed. G. R. Luckhurst and T. J. Sluckin, John Wiley & Sons, 2015) Chap. 2, pp. 265–275.

[42] T. B. T. To, T. J. Sluckin, and G. R. Luckhurst, Liq. Cryst. **43**, 1448 (2016), http://dx.doi.org/10.1080/02678292.2016.1181214.

[43] M. A. Cotter, Mol. Cryst. Liq. Cryst. **39**, 173 (1977), http://dx.doi.org/10.1080/15421407708083918.

[44] D. A. Dunmur, A. Fukuda, and G. R. Luckhurst (eds.), Physical Properties of Liquid Crystals: Nematics, 25 (INSPEC IET, London, 2001).

[45] A. Ferrarini, G. R. Luckhurst, P. L. Nordio, and S. J. Roskilly, Liq. Cryst. **21**, 373 (1996), http://dx.doi.org/10.1080/02678299608032846.

[46] C. G. Gray and K. E. Gubbins, Theory of Molecular Fluids (OUP, New York, 1984).

[47] M. A. Bates and G. R. Luckhurst, Phys. Rev. E **72**, 051702 (2005).

[48] G. R. Luckhurst, C. Zannoni, P. L. Nordio, and U. Segre, Mol. Phys. **30**, 1345 (1975), http://dx.doi.org/10.1080/00268977500102881.

[49] A. Kloczkowski and G. R. Luckhurst, Liq. Cryst. **3**, 95 (1988), http://dx.doi.org/10.1080/02678298808086352.

[50] B. Mulder, Phys. Rev. A **39**, 360 (1989).

[51] P. J. Flory, Macromolecules **7**, 381 (1974), http://dx.doi.org/10.1021/ma60039a022.

[52] J. Katriel, G. F. Kventsel, G. R. Luckhurst, and T. J. Sluckin, Liq. Cryst. **1**, 337 (1986), http://dx.doi.org/10.1080/02678298608086667.

[53] G. R. Luckhurst, Liq. Cryst. **32**, 1335 (2005), http://dx.doi.org/10.1080/02678290500423128.

[54] C. Greco, G. R. Luckhurst, and A. Ferrarini, Soft Matter **10**, 9318 (2014).

[55] D. A. Paterson, M. Gao, Y.-K. Kim, A. Jamali, K. L. Finley, B. Robles-Hernandez, S. Diez-Berart, J. Salud, M. R. de la Fuente, B. A. Timimi, H. Zimmermann, C. Greco, A. Ferrarini, J. M. D. Storey, D. O. Lopez, O. D. Lavrentovich, G. R. Luckhurst, and C. T. Imrie, Soft Matter **12**, 6827 (2016).

[56] A. A. Dawood, M. C. Grossel, G. R. Luckhurst, R. M. Richardson, B. A. Timimi, N. J. Wells, and Y. Z. Yousif, Liq. Cryst. **43**, 2 (2016), http://dx.doi.org/10.1080/02678292.2015.1114158.

[57] C. T. Archbold, E. J. Davis, R. J. Mandle, S. J. Cowling, and J. W. Goodby, Soft Matter **11**, 7547 (2015).

[58] A. A. Dawood, M. C. Grossel, G. R. Luckhurst, R. M. Richardson, B. A. Timimi, N. J. Wells, and Y. Z. Yousif, Liq. Cryst. **44**, 106 (2017), http://www.tandfonline.com/doi/pdf/10.1080/02678292.2017.1290576.

[59] C. Meyer and I. Dozov, Soft Matter **12**, 574 (2016).

[60] W. L. McMillan, Phys. Rev. A **4**, 1238 (1971).